AFRL-RX-WP-TP-2012-0370

COARSENING BEHAVIOR OF GAMMA PRIME PRECIPITATES AND CONCURRENT TRANSITIONS IN THE INTERFACE WIDTH IN Ni-14 AT%A1-7 AT %CR (PREPRINT)

J. Tiley
Metals Branch
Structural Materials Division

S. Meher, T. Rojhirunsakool, J.Y. Hwang, S. Nag, and R. Banerjee
University of North Texas

August 2012
Interim

AIR FORCE RESEARCH LABORATORY
MATERIALS AND MANUFACTURING DIRECTORATE
WRIGHT-PATTERSON AIR FORCE BASE, OH 45433-7750
AIR FORCE MATERIEL COMMAND
UNITED STATES AIR FORCE

REPORT DOCUMENTATION PAGE

Form Approved
OMB No. 0704-0188

1. REPORT DATE *(DD-MM-YY)*	2. REPORT TYPE	3. DATES COVERED *(From - To)*
August 2012	Technical Paper	1 July 2012 – 1 August 2012

4. TITLE AND SUBTITLE

COARSENING BEHAVIOR OF GAMMA PRIME PRECIPITATES AND CONCURRENT TRANSITIONS IN THE INTERFACE WIDTH IN Ni-14 AT%A1-7 AT %CR (PREPRINT)

5a. CONTRACT NUMBER
FA8650-08-C-5226

5b. GRANT NUMBER

5c. PROGRAM ELEMENT NUMBER
62102F

6. AUTHOR(S)

J. Tiley (RXCM)
S. Meher, T. Rojhirunsakool, J.Y. Hwang, S. Nag, and R. Banerjee (University of North Texas)

5d. PROJECT NUMBER
4347

5e. TASK NUMBER

5f. WORK UNIT NUMBER
LM114100

7. PERFORMING ORGANIZATION NAME(S) AND ADDRESS(ES)

University of North Texas
Corner of Avenue C Chestnut
Denton, TX 76203

8. PERFORMING ORGANIZATION REPORT NUMBER

9. SPONSORING/MONITORING AGENCY NAME(S) AND ADDRESS(ES)

Air Force Research Laboratory
Materials and Manufacturing Directorate
Wright-Patterson Air Force Base, OH 45433-7750
Air Force Materiel Command
United States Air Force

10. SPONSORING/MONITORING AGENCY ACRONYM(S)
AFRL/RXCM

11. SPONSORING/MONITORING AGENCY REPORT NUMBER(S)
AFRL-RX-WP-TP-2012-0370

12. DISTRIBUTION/AVAILABILITY STATEMENT

Approved for public release; distribution unlimited. Preprint to be submitted to Scripta Materialia.

13. SUPPLEMENTARY NOTES

The U.S. Government is joint author of this work and has the right to use, modify, reproduce, release, perform, display, or disclose the work. PA Case Number and clearance date: 88ABW-2012-2628, 7 May 2012. This document contains color.

14. ABSTRACT

Coupling atom probe tomography (APT) and transmission electron microscopy (TEM), the temporal evolution of the precipitate morphology and size distribution, and compositional width of γ/γ' interface and associated elemental partitioning, has been tracked in a model Ni-14Al-7Cr(at%) alloy, during isothermal annealing at 8000C. During the initial annealing period, accelerated growth of γ' is accompanied by a gradual decrease in interface width and enhancement of solute partitioning. Further annealing exhibits classical LSW coarsening with minimal changes in the interface.

15. SUBJECT TERMS

Coarsening; Interface; Nickel superalloy; TEM; APT

16. SECURITY CLASSIFICATION OF:			17. LIMITATION OF ABSTRACT:	NUMBER OF PAGES	19a. NAME OF RESPONSIBLE PERSON (Monitor)
a. REPORT	b. ABSTRACT	c. THIS PAGE			Jaimie Tiley
Unclassified	Unclassified	Unclassified	SAR	14	19b. TELEPHONE NUMBER *(Include Area Code)* N/A

Coarsening behavior of Gamma Prime Precipitates and Concurrent Transitions in the Interface Width in Ni-14 at%Al-7 at%Cr

S. Meher, T. Rojhirunsakool, J.Y. Hwang, S. Nag, J. Tiley*, R. Banerjee

Center for Advanced Research and Technology and Department of Materials Science and Engineering
University of North Texas, Denton TX, U.S.A.
*Air Force Research Laboratory, Dayton, OH, U.S.A.

Abstract

Coupling atom probe tomography (APT) and transmission electron microscopy (TEM), the temporal evolution of the precipitate morphology and size distribution, and compositional width of γ/γ' interface and associated elemental partitioning, has been tracked in a model Ni-14Al-7Cr(at%) alloy, during isothermal annealing at 800^0C. During the initial annealing period, accelerated growth of γ' is accompanied by a gradual decrease in interface width and enhancement of solute partitioning. Further annealing exhibits classical LSW coarsening with minimal changes in the interface.

Keywords: Coarsening; Interface; Nickel superalloy; TEM; APT

Paper

Nickel base superalloys typically consist of thermodynamically stable coherent $L1_2$-ordered γ' precipitates in a disordered FCC γ matrix. The change in morphology and size distribution of the precipitates due to exposure to high temperature impacts their mechanical properties [1].The coarsening behavior of γ' precipitates during service is vital for mechanical properties and extensive research work has been done to determine the mechanism and kinetics of this coarsening process [2-10]. The classical coarsening theory developed by Lifshitz-Slyozov[2] and independently by Wagner [3] collectively known as the LSW theory, assumes solute diffusivity within the parent matrix as the rate-limiting step and also assumes no precipitate-precipitate interactions. Local phenomenon like coalescence of precipitates to decrease the interfacial area during growth can be observed in an alloy with high volume fraction of precipitates. Davies et al. modified the basic mean-field nature of the LSW theory and developed Lifshitz-Slyozov encounter modified (LSEM) [4] theory with the assumption of instantaneous coalescence of particles due to overlapping of their diffusion field during growth, resulting in a modification of the basic LSW rate law with a volume dependent rate constant and a broader particle size distribution. Developing a better mechanistic understanding of coarsening critically depends on a more detailed understanding of the precipitate/matrix interface since fundamentally, the total reduction of interfacial and elastic energy is the thermodynamic driving force for coarsening. Most previous phase-field simulations of coarsening kinetics have employed a computed interface width rather than a directly measured physical width [11,12] Recently, Wen et al. [13] have incorporated local effects like dynamically changing composition in the γ/γ'interface region to model the coalescence kinetics in a Ni-Al-Cr alloy. The rate of solute diffusivity across the γ/γ' interface can also change the coarsening mechanism, as recently

proposed in the trans-interface diffusion controlled (TIDC) coarsening model [5]. The application and relevance of the TIDC model[5] is critically dependent on a detailed understanding of the nature of structural and compositional transitions across the interface as highlighted in recent studies using high-resolution scanning transmission electron microscopy (HRSTEM) and atom probe tomography (APT)[14].Over the years there have been a number of detailed investigations of the early stages of γ' precipitation in nickel base superalloys using APT and these have been summarized in some excellent review articles [15-17]. Recently, Hwang et. al has discussed quantitative information on chemical partitioning of alloying elements[18] and interface width [19] in the commercially used Rene 88 DT alloy, using APT. More recently, Ardell[20] has discussed the calculation of the width of coherent γ/γ' interfaces from diffuse concentration profiles across the interface, using the concept of a gradient energy term, originally developed by Cahn and Hilliard [21].APT investigations can be used to accurately determine the width of these diffuse concentration profiles and consequently permits a comparison with values predicted based on the gradient energy term. The present experimental study couples the dynamically changing width and composition profile across the γ/γ' interface with the kinetics of growth and coarsening of γ' precipitates during ageing of Ni-14Al-7Cr (at%) alloy, with a high γ' volume fraction.

The as-cast Ni-14at%Al-7at%Cr alloy was homogenized at 1200^0C for 30 min followed by water quenching. Quartz encapsulated samples with argon atmosphere were aged for 0.25, 1, 4, 16, 64,256hrs at 800^0C and finally water quenched. Transmission electron microscopy(TEM) samples were prepared from mechanically polished 3mm disk samples, subsequently reduced to 20 μm thickness using a dimple grinder, and finally argon ion milled using a Fishione Model 1010 system. The centered dark field images were obtained using a FEI Tecnai F20 microscope operating at 200 kV. Precipitate sizes and circularity values were obtained by applying standard protocols to these images using the IMAGE J software. APT samples were prepared with an apex diameter ~70 nm using a dual-beam focused ion beam (FIB) instrument, the FEI FESEM NOVA 200. The APT experiments were carried out using a CAMECA local electrode atom probe (LEAP^{TM}3000X) system from in the laser evaporation mode at a temperature of 35 K, with the evaporation rate at 0.5%, pulse energy of 0.3 nJ and pulse frequency of 160 kHz. Data analysis was performed using the IVAS 3.6 software.

The centered dark field TEM images of typical γ+γ'microstructures observed in the Ni-14Al-7Cr(at%) alloy, after isothermal annealing at 800°C for various time periods, are shown in Fig. 1.An accelerated growth and coarsening of spherical γ'precipitates is clearly visible in the early stages of annealing (Fig.1 (a), (b)and (c)).Upon further annealing, the morphology tends change towards a cuboidal type with spherical edges as shown in Figs. 1(d),(e) and (f). This change in morphology can be attributed to the anisotropic elastic properties of these precipitates, resulting in a strong spatial alignment along elastically soft <100> direction, as described in detail elsewhere [22].The precipitate size distributions (PSD), for four of the annealing time periods, measured using multiple dark-field images for each case (using the IMAGE J software), have been summarized in Fig. 2(a-d). The number of precipitates used in these analyses ranged from 50-100. Additionally, a comparison of the average precipitate sizes and circularity values, as a function of annealing time, is given in Table 1.

The average precipitate sizes for different annealing time period have been plotted on a plot of radius (r) vs. time ($t^{1/3}$) as shown in Fig. 2(e) to determine if the coarsening of these precipitates follows a classical time-dependent LSW power law expression [2, 3] as given by

$$r_t^3 - r_0^3 = k.t$$

where r_t is the mean particle size at time t,r_0 is the mean particle size at t = 0 and *k*=coarsening rate constant .A linear fit of the experimental data, shown in the r vs. $t^{1/3}$ plot in Fig. 2(e), yields a slope of 1.1 that translates to $k = 1.33 \times 10^{-27} m^3/sec$. Based on the classical LSW model, the value of this rate constant considering diffusion of Al in the matrix as the rate limiting step has been calculated using the following equation:

$$k = \frac{A.D.\sigma.C_e.V_m}{RT}.10^{27}$$

where D is the diffusion coefficient of Al in the matrix at $800^0C = 1x10^{-17} m^2s^{-1}$[23],$C_e$ is the atomic fraction of Al in equilibrium with the precipitate=0.08(from Table 2),σ is the precipitate/matrix interface energy $=30 \times 10^{-3}$ J/m^2[24],V_m is the molar volume of the precipitate $=2.716x10^{-5}$ m^3mol^{-1}[25],R is the universal gas constant=8.31$Jmol^{-1}K^{-1}$and T is the absolute temperature=1073 K.Putting all these values in the above mentioned equation gives the value of *k* to be 0.37×10^{-27} m^3/sec, that is in reasonable agreement with the experimental determined value noted above. The difference between these two values of *k* can be possibly attributed to the inaccuracies associated with the values of D, σ, as well as the measurement of the precipitate sizes from the TEM dark-field images .It should be noted that while the points on the plot shown in Fig. 2(e), corresponding to the longer annealing time periods, are in good agreement with the linear fit, the temporal power law exponent has been calculated to be 0.318 from a log r vs. log t plot, and consequently appear to follow classical LSW coarsening. The two points corresponding to the early stage of annealing show substantial departure from the LSW prediction. Therefore, it appears that there is a period of rapid increase in the average precipitate size at the early stages of annealing that can be attributed to a combined growth and coarsening phase during these early stages. According to the LSW model, the maximum allowed normalized PSD is 1.5. Excluding the early stage of annealing, i.e. at 0.25 hr showing a maximum normalized PSD value of 1.76 (refer to Fig. 2(a)), for longer annealing times, these values range from 1.5 to 1.6, which is very close to the allowed upper limit based on the LSW model. The high value of PSD at 0.25 hr can be attributed to high degree of precipitate coalescence, broadening its tail. So it is conclusive from time invariant PSDs onwards 1 hr of annealing that the matrix diffusion limited microstructural evolution is self-similar.

Two atom probe reconstructions of this alloy for the as-quenched and 0.25 hr annealed conditions are shown in Figs. 3(a) and (b) respectively. These reconstructions show the Al-rich γ' precipitates, delineated by Al iso-concentration (14 at%) surfaces, together with Ni ions. The precipitates appear to be interconnected in both these reconstructions suggesting a tendency for coalescence during growth and coarsening. The Al and Cr composition profiles, corresponding to the 14at% Al isosurface, for all the annealing conditions have been shown in Fig. 4 as proximity histograms or proxigrams [26,27], generated using the IVAS™ reconstruction software. The elemental partitioning across the γ/γ' interface and the compositional width, corresponding to Al partitioning, have also been summarized in Table 2.Additionally, local and far-field γ matrix compositions for the different annealing times have been included in the same table. The compositional width of the interface has been estimated based on the approach suggested by

Ardell [20]. The model defines the interface width as $\delta = \Delta X/(dX/dZ)_{max}$ where ΔX=difference in steady state composition of γ and γ'and $(dX/dZ)_{max}$is the maximum slope of the diffuse interface. The values of ΔX and $(dX/dZ)_{max}$ have been determined from the APT data. The model proposed by Ardell [20] also suggests that the onset of coarsening corresponds to when the compositional width of the interface reaches a steady-state value if ΔX remains constant. Analyzing the data shown in Table 2, clearly shows that the γ/γ' interface width reaches a steady-state value of ~2 nm for annealing time periods longer than 1 hr, as well as there is no temporal change in matrix composition. These observations suggest that a pure coarsening regime is initiated for time periods greater than 1 hr.

The quantitative data shown in Table 2 and the proxigrams shown in Fig. 4 substantiate this clear distinction between the early stages (time period from 0 to 1 hr) where concomitant growth and coarsening occurs, and the later stages from 4hrs to 256 hrs where steady-state coarsening appears to take place. Table 2 shows that the interface width changes from 3.5 nm to 2.5 nm during the early stages of annealing. At the same time the Al content in the γ matrix decreases from 9.5 to 8.6 at% with increasing distance from the γ/γ' interface. This gradual change in matrix composition is an indication of far-field non-equilibrium compositions. The compositionally diffuse nature of the interface coupled with the high volume fraction of γ', results in rather small inter-precipitate distances, favoring local phenomena like coalescence of precipitates to decrease interfacial energy. The opposite trend can be observed in case of the Cr composition profile as shown in Fig. 4 as well as reflected in the values in Table 2. These results indicate that local effects associated with the interface, such as elemental partitioning and variation in the compositional width, are responsible for the high degree of precipitate coalescence, leading to a high rate of increase in precipitate size during the early stages. Zhu et al.[11] has discussed the accelerated coalescence of neighboring γ' precipitates with large interface widths based on simulation studies .Additionally, previous experimental studies [28] have also reported a higher coarsening rate than that predicted by the LSW model, due to coalescence. The present experimental studies also exhibit a transient depletion of Al, and enrichment of Cr, adjacent to the γ/γ' interface, during the early stages of annealing, as shown in Figs. 4(a), (b) and (c) and listed in Table 2. These transient compositional effects can be attributed to diffusion-limited growth as explained elsewhere[29].Also, the gradual increase in solute partitioning across the γ/γ' interface, with annealing time, affects the misfit between these two phases and the resultant strain energy, and consequently the circularity values change as shown in Table 1.

Here, a strong influence of experimentally tracked non-equilibrium γ/γ' interface profile on coarsening has been discussed in contrast to simulations where extrapolated value from thermodynamic equilibrium values are used for early stage of coarsening.

- During early stage of annealing in Ni-14Al-7Cr(at%), the accelerated growth of γ' has been attributed to the gradual decrease in compositional width of γ/γ' interface from 3.5 nm to 2.5 nm and continuously changing solute partitioning across the interface with transient depletion of Al and enrichment of Cr at interface.
- During later stage of annealing, the interface width remains constant with no compositional change in matrix which indicates the onset of classical LSW coarsening with k= 1.33 x$10^{-27}$$m^3$/sec and temporal growth exponent =0.318.

To understand the influence of γ/γ' interface on complete domain of growth and coarsening by varying volume fraction and temperature is a subject of future research.

References

[1] Reed RC. The superalloys, fundamentals and applications.Cambridge:Cambridge University Press; 2006.
[2] Lifshitz IM, Slyozov VV. J PhysChem Solids 1961;19:35.
[3] Wagner C. Z Elektrochem 1961;65:581.
[4]Davies CKL,NashP,Stevens RN ,ibid,28(1980)179
[5] Ardell AJ, Ozolins V. Nat Mater 2005;4:309.
[6]Ardell AJ. Acta Metall 1972;20:61
[7]Ardell AJ, Nicholson RB. J PhysChem Solids 1966;27:1793
[8]Voorhees PW. J Stat Phys 1985;38:231.
[9] McLean D. Metal Sci 1984;18:249.
[10]Ardell AJ. Scripta Metall Mater 1990;24:343
[11]Zhu JZ, Wang T, Ardell AJ, Zhou SH, Liu ZK and Chen LQ Acta Mater2004;52:2837-45
[12] Kim SG, Kim WT, Suzuki T,Phys Rev E 1999;60:7186.
[13] Wen YH, Simmons JP, WoodwardC, Modelling Simul. Mater. Sci. Eng. 18 (2010)
[14] Srinivasan R, Banerjee R, Hwang JY, Viswanathan GB, TileyJ,Fraser HL. Phys Rev Lett 2009;102:086101.
[15] Blavette D, Cadel E, Deconihout B, Mater Charact2000;44:133–57
[16] Miller MK. Micron 2001;32: 757–64
[17] Seidman DN, Sudbrack CK, Yoon KE,JOM 2006;58: 34–9.
[18] Hwang JY, Banerjee R, Tiley J, Srinivasan R, Viswanathan GB, Fraser HL, Metall. Mater. Trans. A 40 (2009) 24
[19] Hwang JY, Nag S, Singh ARP Srinivasan R, Tiley J,Fraser HL and Banerjee R, Scripta Mater. 61 (2009) 92–95
[20]Ardell AJ. Scripta Mater. 66(2012)423-426
[21]Cahn JW, HilliardJE,J. Chem. Phys.28(1958)258
[22] Wang Y, Khachaturyan AG. Acta Metall Mater 1995;43:1837.
[23]Gale WF,Totemeier TC, Smithell's handbook. 8th ed. Oxford: Butterworth-Heinemann; 2004
[24]Ardell AJ,J Mater Sci (2011) 46:4832–4849
[25]McLean D. Metal Sci 1984;18:249.
[26] Yoon KE, NoebeRD, HellmanOC and Seidman DN.Surf. Interface Anal., 36 (2004), p. 594
[27] Miller MK. Surf. Int. Anal., 31 (2001), p. 593
[28]Hoopgood AA and Martin JW, ibid. 2 (1986) 543.
[29] Sudbrack CK, Noebe RD, Seidman DN, Solid-Solid Phase Transformations in Inorganic Materials, 2:543(2005)

Figure Captions

Figure 1

Centered Dark field micrographs showing γ' in Ni-14Al-7Cr(at%), isothermally aged at 800°C for (a) 0 hr (b)0.25 hr (c) 1 hr (d) 16 hrs (e) 64 hrs (f) 256 hrs conditions

Figure 2

Particle size distribution for different ageing time (a) 0.25hr (b) 1 hr (c) 4 hrs (d) 256 hrs and (e) Linear fit of precipitate size(nm) vs. cube root of annealing time

Figure 3

APT reconstruction delineated with 14% Al iso-surface showing coalescence of γ' in Ni-14Al-7Cr(at%) isothermally aged at 800°C for (a) 0 hr (b)0.25 hr

Figure 4

Composition profile and interface width across γ/γ' in Ni-14Al-7Cr(at%) annealed at 800°C for (a) 0 hr(b)0.25 hr (c) 1 hr (d) 16 hrs (e) 64 hrs (f) 256 hrs

Tables

Table 1.

Comparison of the average γ' precipitate sizes and circularity values for various annealing period

Ageing Time(hr)	Average radius(nm)	Circularity of γ'
0.25	8	0.93
1	25	0.91
4	30	0.81
16	44	0.7
64	75	0.7
256	108	0.6

Table 2.

Comparison of elemental partitioning across the γ/γ' interface and the compositional width for various annealing period

Ageing Time (hr.)	Far field γ comp (at %)		Local equilibrium γ comp (at %)		γ' comp (at %)		Interface width, δ (nm)
	Al	Cr	Al	Cr	Al	Cr	
0	9.5	7.5	9.1	8.4	18.8	5.7	3.5
0.25	9.2	8.7	8.9	8.9	18.2	5.6	3
1	8.6	8.4	8.0	8.6	18	5.6	2.5
4	8	8.5	8	8.5	17.3	5.9	2.1
16	8.3	8.3	8.3	8.3	18	5.8	2.02
64	8.3	8.2	8.3	8.2	17	5.6	2.02
256	8.0	8.5	8.0	8.5	17	5.9	2.02

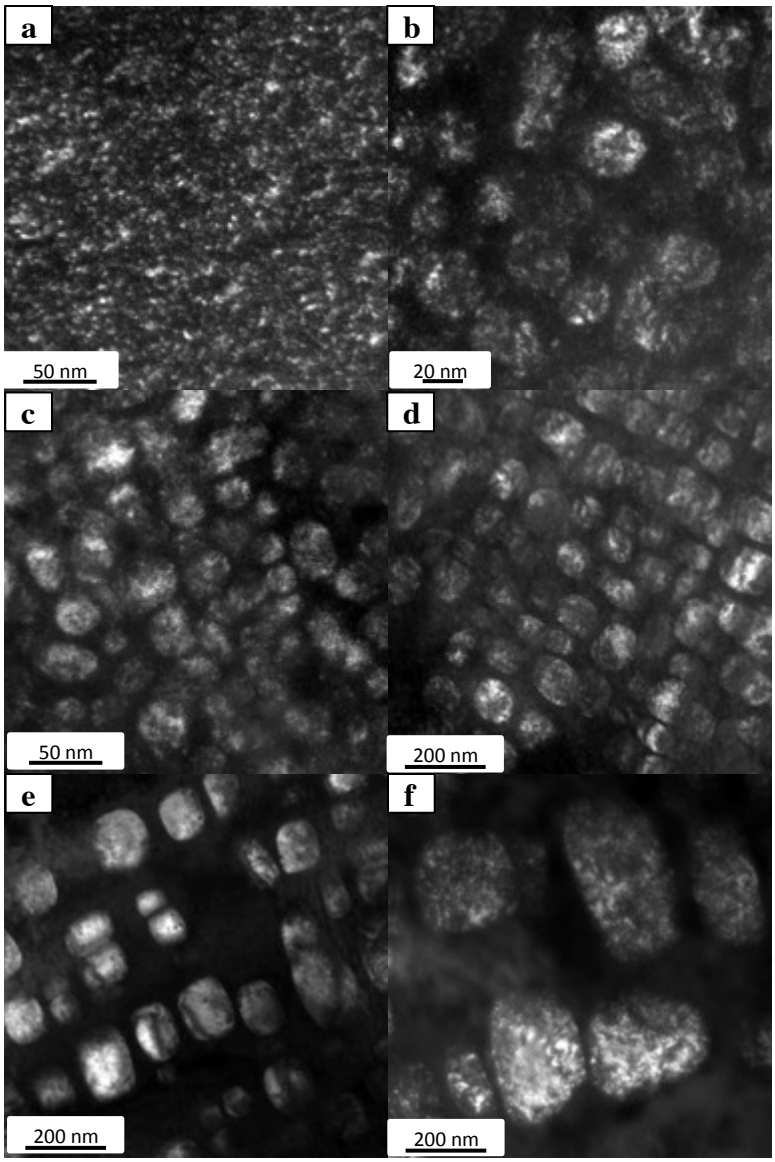

Fig. 1

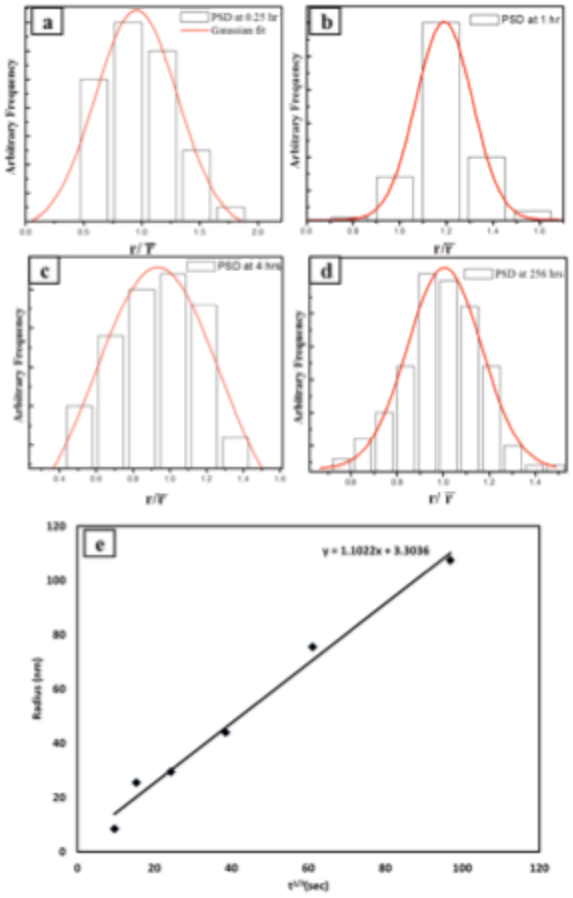

Fig. 2

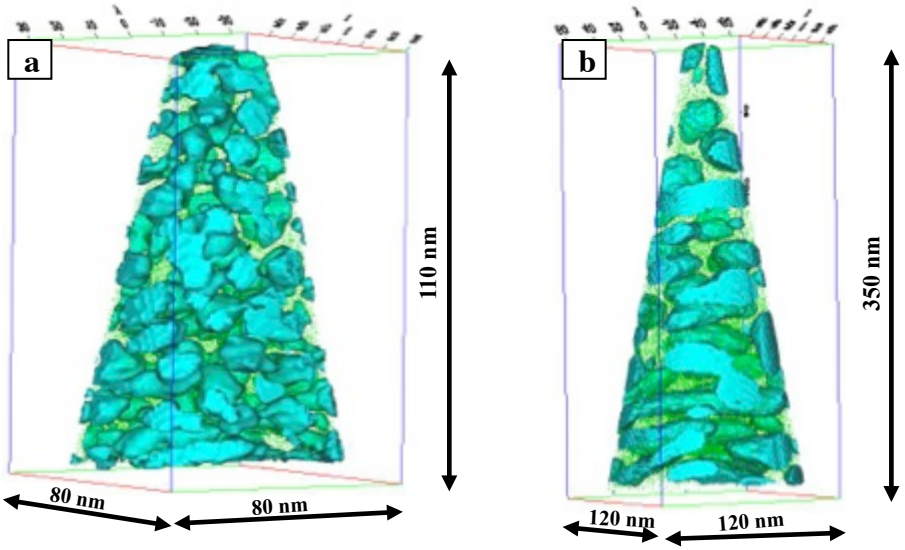

Fig. 3

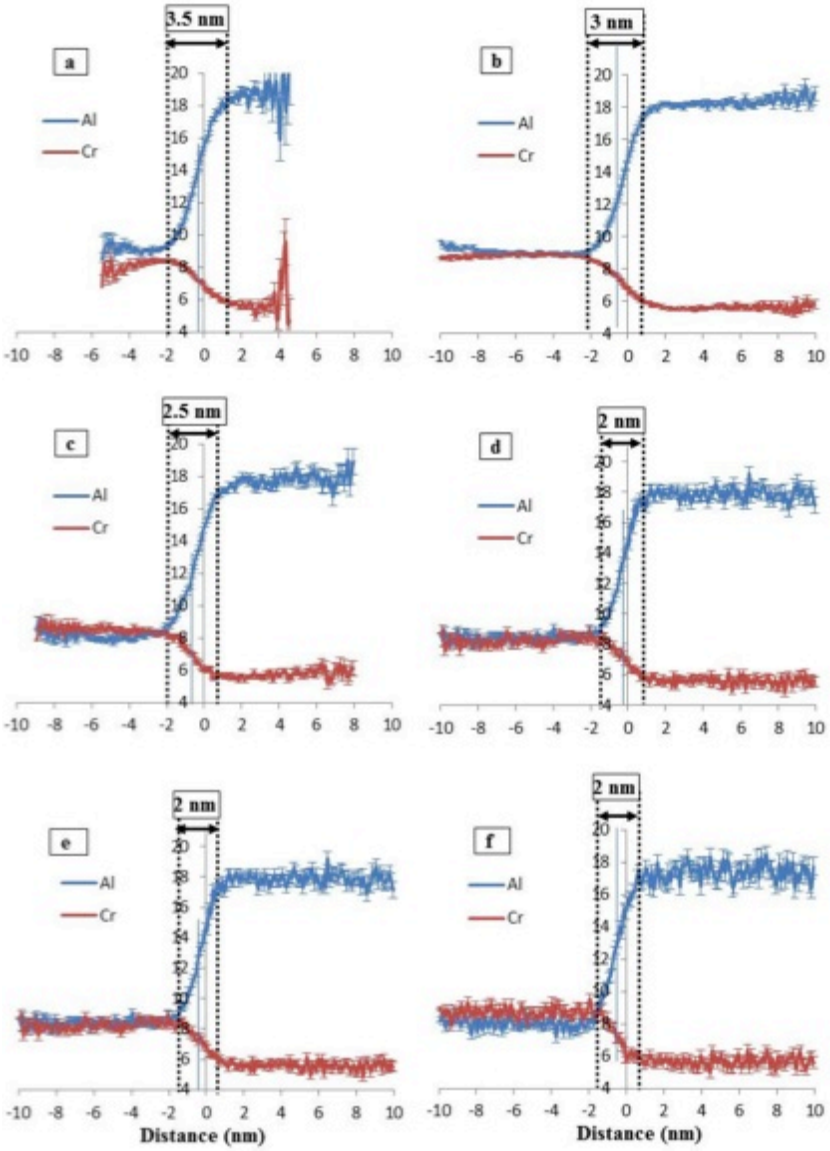

Fig. 4